The Stability of Time-Split Numerical Methods for the Hydrostatic and the Nonhydrostatic Elastic Equations

WILLIAM C. SKAMAROCK AND JOSEPH B. KLEMP

National Center for Atmospheric Research, Boulder, Colorado*

(Manuscript received 12 June 1991, in final form 12 December 1991)

ABSTRACT

The mathematical equivalence of the linearized two-dimensional (2D) shallow-water system and the 2D acoustic-advection system strongly suggests that time-split schemes designed for the hydrostatic equations can be employed in nonhydrostatic models and vice versa. Stability analyses are presented for several time-split numerical methods for integrating the two systems. The primary interest is in the nonhydrostatic system and in explicit numerical schemes where no multidimensional elliptic equations arise; thus, a detailed analysis of the Klemp and Wilhelmson (KW) explicit technique for integrating the time-split nonhydrostatic system is undertaken. It is found that the interaction between propagating and advecting acoustic modes can introduce severe constraints on the maximum allowable time steps. Proper filtering can remove these constraints. Other explicit time-split schemes are analyzed, and, of all the explicit schemes considered, it is believed that the KW time-split method offers the best combination of stability, minimal filtering, simplicity, and freedom from spurious noise for integrating the nonhydrostatic or hydrostatic equations.

Schemes wherein the fast modes are integrated implicitly and the slow modes explicitly are also analyzed. These semi-implicit schemes can be used with a greater variety of advection schemes than the explicit time-split approaches and generally require less filtering than the split-explicit schemes for stability. However, a multidimensional elliptic equation must be solved with each time step.

For nonhydrostatic elastic models using the KW time-split method, an acoustic filter is presented that allows a reduction of previously necessary filtering in the KW scheme, and a method for integrating the buoyancy equation is discussed that results in the large time step being limited by a Courant condition based on the advection velocity and not on the fastest gravity-wave speed.

1. Introduction

Atmospheric motions occur on many time scales, from the rapid propagation of acoustic and gravity waves to the slower-moving Rossby waves and advection. Marchuk (1974) was the first to suggest that time-split methods be used to integrate numerical models of the atmosphere. In his *splitting-up* approach, he proposed integrating the advection, adjustment, and dissipation terms separately using techniques appropriate for the different time scales of these processes. While Marchuk was concerned with solving a hydrostatic system of equations, the use of time-split techniques is similarly attractive for nonhydrostatic modeling.

While time-split techniques are widely used in hydrostatic and nonhydrostatic models, the close conceptual relationship between the hydrostatic models, where the fast signals are gravity waves and the slow signals are the advected modes, and the fully compressible nonhydrostatic models, where the fast signals are sound waves, has not been discussed in presentations of time-split schemes. As a result, schemes have been developed independently for hydrostatic and nonhydrostatic models with little intercomparison of methods. Our primary interest is in further understanding and improving the explicit splitting techniques used in nonhydrostatic models; thus, we are led to consider splitting techniques used in both hydrostatic and nonhydrostatic models.

In the development of new splitting techniques, it is often difficult to assess their stability across the wide range of possible model parameters. In this paper, we present the results of stability analyses for several time-split schemes used in hydrostatic and nonhydrostatic models and also analyze possible extensions to some existing schemes. Traditionally, time-split numerical methods are those wherein different modes in the system are integrated separately, without regard for the other modes (see Marchuk 1974). We examine the more general class of schemes wherein terms responsible for fast modes are integrated in a different manner than the terms responsible for slow modes, but often

* The National Center for Atmospheric Research is sponsored by the National Science Foundation.

Corresponding author address: Dr. William C. Skamarock, NCAR, P.O. Box 3000, Boulder, CO 80307-3000.

in a more tightly coupled manner than in the traditional time-split schemes. Also, while we are most concerned with the computationally more straightforward explicit time-split schemes, we also discuss the single-time-step implicit and semi-implicit schemes.

Our particular interest in nonhydrostatic models extends not only from their past and future use in cloud-scale simulations but in their growing role in the simulation of larger-scale atmospheric motions. While earlier models were used to study convective storms (e.g., Klemp and Wilhelmson 1978; Schlesinger 1978; Clark 1979) and other small-scale phenomena, nonhydrostatic models are now being used to examine large-scale motions, such as baroclinic waves (Polavarapu and Peltier 1990; Snyder et al. 1991), as well as mesoscale weather prediction (Golding 1987). It is also becoming apparent that nonhydrostatic models can be integrated as economically as hydrostatic models at the same resolution, as is demonstrated in Snyder et al. using the split-explicit technique we describe in section 4 of this paper and in Cullen (1990) and Tanguay et al. (1990). The continued development of more sophisticated nested and adaptive models will promote a broader use of the nonhydrostatic equations with an even wider range of motion scales contained in single simulations.

Two equation sets are widely used in nonhydrostatic models: anelastic equations, from which the sound waves have been filtered, and elastic equations, which retain the sound waves. The principal advantage of the anelastic equations is that a reasonably large time step is allowed, the time step being limited by the fastest-propagating gravity wave. However, use of the system requires the solution of a multidimensional elliptic pressure equation with every time step. While fast elliptic solvers exist for simple, uniform grids, the introduction of orography or variable-resolution grids requires the use of iterative solvers or the iterative use of direct solvers (Clark 1977).

Sound waves are not important in atmospheric motions of meteorological interest and their high propagation speed severely restricts the maximum allowable time step in a numerical integration. In cloud modeling, Hill (1974) was the first to use the fully compressible elastic equations where the time step is limited by the sound waves. These integrations are much more costly than integrations of the anelastic equations, and several methods have since been developed to speed the integration of the full-elastic set. Tapp and White (1976) employ an elastic model wherein the terms responsible for the acoustic modes are handled implicitly. A Helmholtz equation for the second time derivative of the pressure is solved using the alternating direction implicit method (ADI; Peaceman and Rachford 1955). Carpenter (1979) introduced terrain into the Tapp and White model in a manner such that the form of the Helmholtz equation does not change; thus, this elliptic equation is easier to solve than the corresponding equation in the anelastic model. Carpenter notes that the Helmholtz equation becomes nonregular with any vertical coordinate system other than the one he employs.

Another approach to integrating the elastic equations involves isolating the terms responsible for the acoustic modes and integrating them with a smaller explicit time step. This time-split approach, first proposed by Klemp and Wilhelmson (1978; hereafter referred to as KW), is appealing because it is computationally much simpler than handling the acoustic modes implicitly or using the anelastic system. The finite-difference equations maintain their simple explicit form and no multidimensional elliptic equations need to be solved, although KW do solve a one-dimensional (1D) Helmholtz equation that arises with the implicit treatment of vertically propagating sound waves. Orography is easily handled in the time-split system, and the choice of variables and coordinate systems is not tied to the time-split method. The computational effort required for integrating the anelastic and elastic systems is roughly equivalent.

The relative simplicity, computational economy, and freedom in the choice of variables and coordinate systems has led many groups to develop nonhydrostatic models based on the KW time-split technique. However, a complete analysis of this time-split system has not been presented, though the general stability of the scheme can be inferred from the analysis of Tatsumi (1983), who examines the scheme in the context of a hydrostatic model, and in the analysis of Ikawa (1988), who is concerned with the effect of orography on scheme stability. The anelastic models, and the elastic models where an explicit time-split technique is not used, lend themselves to relatively straightforward analyses because of their single-time-step approach. For example, Tapp and White (1976) present a stability analysis based on the dispersion relation for the discrete system where sound waves are handled implicitly. For the KW time-split approach, separate analysis of a single small or large time step (acoustic and nonacoustic terms, respectively) are similarly straightforward, and these results are presented in KW, Durran and Klemp (1983; hereafter DK), and others. However, the overall stability of the time-split scheme cannot be extracted by considering the small and large time steps separately; rather, they must be analyzed as a coupled system.

A wider range of time-split schemes has been developed for hydrostatic models than for their nonhydrostatic counterparts. The approach of Marchuk can be more generally termed an *additive-splitting* scheme, and more concrete examples are given by Burridge (1975) and Gadd (1978). The additive-splitting schemes can engender numerical noise in nonlinear and even linear calculations (McGregor 1987; Purser and Leslie 1991), and more sophisticated schemes have been developed to circumvent this problem. We examine the additive-splitting schemes because they have

proven to be very stable (Leveque and Oliger 1983) and can form the basis for new schemes.

More sophisticated splitting approaches are also used in hydrostatic models. Madala (1981) describes a scheme that can be considered an extension of the KW scheme though used in a hydrostatic model. Tatsumi (1983) presents a scheme that is identical to the explicit KW scheme, again for use in a hydrostatic model. Purser and Leslie (1991) present an extension to an additive-splitting scheme that greatly reduces the noise in their computations. Several semi-implicit schemes are also used that possess interesting stability properties.

As noted, the hydrostatic and nonhydrostatic elastic systems can be integrated using the same general splitting techniques. In section 2, we outline a common basis for their analysis. A more complete linearized equation set for nonhydrostatic models will also be presented because of our interest in analyzing the nonhydrostatic systems in more detail. A brief discussion of additive-splitting schemes is given in section 3. In section 4, we present a detailed analysis of the KW time-split approach. Some existing time-split schemes are considered in section 5, along with analyses of several possible new schemes. Conclusions and a brief discussion appear in section 6.

In section 4, we also introduce two new variants to the KW scheme for use in nonhydrostatic elastic models. In particular, we present an acoustic filter based on the concept of divergence damping, and a method for handling the buoyancy term that results in a time step no longer restricted by the buoyancy, an important consideration when using the nonhydrostatic equations for synoptic-scale simulations.

2. Equations

Our stability analyses, like most, focus on a linearized version of the full nonlinear equations. First, consider the linearized equations for the nonhydrostatic elastic system. For a stability analysis of numerical methods for solving the nonhydrostatic elastic system, it is generally sufficient to consider a 2D nonhydrostatic, elastic equation set where a perturbation Exner function takes the place of pressure. The approximate, quasi-Boussinesq, linearized equations are

$$u_t + c_s p_x + U u_x = 0, \tag{1}$$

$$w_t + c_s p_z + U w_x - N\theta = 0, \tag{2}$$

$$\theta_t + Nw + U\theta_x = 0, \tag{3}$$

$$p_t + c_s(u_x + w_z) + U p_x = 0. \tag{4}$$

In these equations, u and w are the horizontal and vertical perturbation velocities, θ is the potential temperature divided by the Brunt–Väisälä frequency N, p is the perturbation Exner function divided by $c_s/(c_p\theta_0)$, c_s is the constant speed of sound, and U is a mean advection velocity. To further simplify the analysis, vertical gradients of mean density are ignored. The advection term Up_x is included in (4). Klemp and Wilhelmson (1978) have alternately retained and discarded this term and find little difference in their simulations. Here the advection of p is kept because it results in a symmetric set of equations that aids the analysis. Results from stability analyses where this term is dropped differ only slightly from those presented here. This linearized set is appropriate for shallow convection and is essentially that derived by Phillips and Ogura (1962), except that compressibility has been retained for computation convenience.

To focus on time-integration methods, the spatial discretizations are ignored at present and the spatial structure of the variables is represented as a sum of continuous Fourier modes,

$$\phi = \sum \hat{\phi}(t) \exp[i(kx + lz)],$$

where k and l are wavenumbers in x and z, respectively. With this representation, (1)–(4) become

$$\hat{u}_t + ic_s k\hat{p} + ikU\hat{u} = 0, \tag{5}$$

$$\hat{w}_t + ic_s l\hat{p} + ikU\hat{w} - N\hat{\theta} = 0, \tag{6}$$

$$\hat{\theta}_t + N\hat{w} + ikU\hat{\theta} = 0, \tag{7}$$

$$\hat{p}_t + ic_s(k\hat{u} + l\hat{w}) + ikU\hat{p} = 0. \tag{8}$$

This is the linearized set we consider when analyzing the stability of time-split numerical methods used in nonhydrostatic elastic models.

In the development of time-split numerical methods for hydrostatic models, the shallow-water system is often used to test the schemes. The extension of a time-split scheme from the shallow-water system to the full baroclinic primitive equations can be performed in several ways, and examples of this extension can be found in Gadd (1978), Madala (1981), Chao (1982), Tatsumi (1983), and several other works. The 2D linearized shallow-water equations used in these analyses can be expressed as

$$u_t + Uu_x + Vu_y + c_g h_x + fv = 0, \tag{9}$$

$$v_t + Uv_x + Vv_y + c_g h_y - fu = 0, \tag{10}$$

$$h_t + c_g(u_x + v_y) + Uh_x + Vh_y = 0, \tag{11}$$

where the horizontal velocities are u and v, c_g is the gravity-wave speed $\sqrt{gH}$, and h is the height of the free surface divided by c_g/g.

Equations (9)–(11) are similar to a 2D acoustic-advection system; the transformation requires replacing c_g with c_s and h with p, and the fast modes are the sound waves in one and gravity waves in another. If we drop the Coriolis terms in (9) and (10), remove the mean velocity V in (9)–(11), and drop the potential temperature θ in (1)–(4), then the nonhydrostatic system in x, z coordinates is identical to the shallow-

water system in x, y coordinates. The Coriolis terms in (9) and (10) do not significantly affect the stability of schemes in most hydrostatic calculations, and the buoyancy terms in (1)–(4) are easily incorporated into time-split schemes in such a way as they do not adversely affect scheme stability [see section 4d; Cullen (1990); or Tanguay et al. (1990)].

The major stability constraints in both systems arise from the sound in the nonhydrostatic system and gravity waves in the hydrostatic system. Thus, the general equivalence of the two systems implies that splitting schemes applied to one system could be directly applicable to the other. Given this relationship, we analyze the stability of time-split schemes in the context of the nonhydrostatic system (1)–(4) in this paper, with the understanding that the analyses also apply to the schemes used for solving the hydrostatic system.

In the next four sections we examine the stability of various time-split schemes for integrating (1)–(4), or numerical schemes for integrating (9)–(11) applied to (1)–(4). For $N \geq 0$, the continuous equations (1)–(4) admit wave-type solutions that do not exhibit exponential growth; hence, numerical schemes for solving (1)–(4) are deemed stable when solutions to the discretized equations do not grow. Two general stability analyses will be used. In the von Neumann stability analysis, the discretized system is written as $\phi_{n+1} = A\phi_n$ and the numerical scheme is stable when the amplification factor A, or the eigenvalues of the amplification matrix $\mathbf{A}$ (for systems with more than one dependent variable), have an absolute value less than or equal to one. Further details concerning von Neumann stability analysis can be found in the Appendix and in Roache (1972). The second stability analysis, in the spirit of traditional ordinary differential equation (ODE) analyses, requires determining the dispersion relation for the discrete system by assuming solutions of the form $\phi = \exp(-i\omega t)$, where the frequency ω is always real for solutions to the continuous set. The discretized equations are stable when $\mathrm{Im}(\omega) \leq 0$; $\mathrm{Im}(\omega) > 0$ results in exponential growth.

3. Methods based on additive splittings

The most straightforward time-split approach is that based on additive splittings. Marchuk (1974) was the first to suggest that additive-splitting methods be used for atmospheric computations, and called it the *splitting-up* method. In this approach, analyzed in detail by Leveque and Oliger (1983), the 1D advection-acoustic-mode system (1) and (4) is written as

$$\mathbf{u}_t = -\underbrace{\begin{pmatrix} U & 0 \\ 0 & U \end{pmatrix}}_{A_s}\mathbf{u}_x - \underbrace{\begin{pmatrix} 0 & c_s \\ c_s & 0 \end{pmatrix}}_{A_f}\mathbf{u}_x, \qquad (12)$$

where the slow modes are contained in A_s, the fast modes are contained in A_f, and $\mathbf{u}$ is the solution vector (u, p). The original system is recovered by adding the matrices multiplying $\mathbf{u}_x$, hence Leveque and Oligers' and our use of the descriptive term *additive splittings.*

The additive-splitting method seeks the solution to the system (12) by alternating between the solution of two simpler systems:

$$\mathbf{u}_t = -A_s\mathbf{u}_x, \qquad (13a)$$

$$\mathbf{u}_t = -A_f\mathbf{u}_x. \qquad (13b)$$

By defining a discrete solution vector $\mathbf{u}_m^n$ at the discrete time n and spatial point m and defining two discrete operators Q_f and Q_s that advance the solution vector one time interval for the fast and slow modes, that is, for the fast modes [(13a)]

$$\mathbf{u}_m^{n+1} = Q_f(\Delta t)\mathbf{u}_m^n,$$

and for the slow modes [(13b)]

$$\mathbf{u}_m^{n+1} = Q_s(\Delta t)\mathbf{u}_m^n,$$

the solution to the system containing both the fast and slow modes [(12)] can be obtained by applying these operators in sequence to the solution vector $\mathbf{u}$:

$$\mathbf{u}_m^{n+1} = Q_s(\Delta t)Q_f(\Delta t)\mathbf{u}_m^n. \qquad (14)$$

Two approaches have been used in applying the splitting (14) to the shallow-water or primitive equations. Gadd (1978) and others have defined the operator advancing the fast modes to be

$$Q_f(\Delta t) = Q_{f*}^M\left(\frac{\Delta t}{M}\right),$$

where the operator Q_{f*} denotes an explicit integration of the fast modes, and M time steps of $\Delta t/M$ are used to advance the solution vector. In the other approach, the operator advancing the fast modes denotes an implicit integration or possibly an ADI scheme (e.g., Bates 1984).

Leveque and Oliger show that the stability of the individual operators Q_f and Q_s does not always ensure overall stability for the time-split method because scheme stability is intimately tied to the coupling between the slow and fast modes in the system. However, the system (12) is symmetric, and Leveque and Oliger have shown that for symmetric systems the solution procedure is stable when the fast- and slow-mode operators are stable (a more general result is given in Leveque and Oliger). The stability analysis assumes the use of single–time-level schemes (for example, Lax–Wendroff) as opposed to multiple–time-level schemes (for example, leapfrog). The stability analysis by Gadd, and the experiences of Bates and McDonald (1982) and others, lend practical evidence for Leveque and Oliger's result. Also of interest is that both analysis and experience suggest that the use of multiple–time-level schemes is problematic in this splitting approach.

McGregor (1987), Purser and Leslie (1991), and others note that the additive splitting (14) can contribute significantly to the problems of spurious noise in linear and, more importantly, in nonlinear calculations. The splitting (14) is only first-order accurate in time. Strang (1968) gives a second-order–accurate counterpart to (14):

$$\mathbf{u}_m^{n+1} = Q_f\left(\frac{\Delta t}{2}\right) Q_s(\Delta t) Q_f\left(\frac{\Delta t}{2}\right) \mathbf{u}_m^n.$$

This splitting significantly reduces the noise in McGregor's calculations. Unfortunately, the splitting errors can still be large (see Purser and Leslie's examples). No models based on additive-splitting methods are used for nonhydrostatic calculations, and very few are still used for hydrostatic computations.

In the additive-splitting approach the slow and fast modes are integrated separately. In the next three sections, we will consider methods whereby, while the slow and fast modes are still split in the sense that they are integrated with different methods, the modes are integrated simultaneously in a more tightly coupled manner. These methods have been developed as a means of reducing the splitting error and the attendant noise in additive time-split models.

4. Stability of the KW time-split method

The KW time-split scheme is similar to the explicit additive-splitting methods in that terms responsible for the acoustic modes are integrated with an explicit time step that is smaller than the time step used for the advection and gravity-wave terms. However, KW integrates the slow and fast modes simultaneously, as opposed to separately as in the additive-splitting methods.

The KW method uses a leapfrog time-integration scheme for the slow modes, and in previous presentations of the time-split scheme the buoyancy equation (7) is integrated with the leapfrog time step Δt using the discretization

$$\theta^{t+\Delta t} = \theta^{t-\Delta t} - \lambda_N w^t - i\lambda_u \theta^t, \tag{15}$$

where $\lambda_u = 2\Delta t k U$ and $\lambda_N = 2\Delta t N$. The carat ($\hat{}$) is dropped over the Fourier variables for the remainder of the paper, and all variables with the time superscripts refer to transformed variables except where noted.

The remaining equations, (5), (6), and (8), are advanced with n_s small time steps $\Delta\tau$ from $t - \Delta t$ to $t + \Delta t$, where $n_s = 2\Delta t/\Delta\tau$. Acoustically inactive terms in the equations are evaluated using values at time t and held fixed over the n_s small time steps. The discretizations for the small time step equations as given in KW are

$$u^{\tau+\Delta\tau} = u^\tau - i\lambda_{cx} p^\tau - \frac{i}{n_s}\lambda_u u^t, \tag{16}$$

$$w^{\tau+\Delta\tau} = w^\tau - \frac{i\lambda_{cz}}{2}(p^{\tau+\Delta\tau} + p^\tau) - \frac{i}{n_s}\lambda_u w^t + \lambda_N \theta^t, \tag{17}$$

$$p^{\tau+\Delta\tau} = p^\tau - \frac{i\lambda_{cz}}{2}(w^{\tau+\Delta\tau} + w^\tau) - i\lambda_{cx} u^{\tau+\Delta\tau} - \frac{i}{n_s}\lambda_u p^t, \tag{18}$$

where $\lambda_{cx} = \Delta\tau c_s k$ and $\lambda_{cz} = \Delta\tau c_s l$. Finally, a time filter is applied to variables at the large-time-step intervals to keep the time levels coupled (Robert 1966):

$$\phi^t = \phi^t_* + \alpha(\phi^{t-1} - 2\phi^t_* + \phi^{t+1}_*),$$

where the asterisk (*) designates variables that have not yet been smoothed. Next the stability of this method is considered.

a. *Stability analysis for explicit differencing*

The interaction between horizontally propagating acoustic modes and advection is responsible for the most severe stability constraints in the KW time-split method. These constraints can be examined in one spatial dimension by an analysis of the discretized equations (16) and (18). In one dimension, the relevant untransformed continuous equations (1) and (4) become

$$u_t + c_s p_x + U u_x = 0, \tag{19}$$

$$p_t + c_s u_x + U p_x = 0, \tag{20}$$

and the transformed discretized equations are

$$u^{\tau+\Delta\tau} = u^\tau - i\lambda_{cx} p^\tau - \frac{i}{n_s}\lambda_u u^t \tag{21}$$

$$p^{\tau+\Delta\tau} = p^\tau - i\lambda_{cx} u^{\tau+\Delta\tau} - \frac{i}{n_s}\lambda_u p^t. \tag{22}$$

First, consider the non–time-split system, that is, $n_s = 1$. The discrete system is pure leapfrog for advection, and forward–backward time differencing is used for the terms multiplied by c_s (Mesinger 1977). This method is stable for $|\lambda_u \pm \lambda_{cx}| \leq 2$. In contrast, for acoustic modes alone, stability of the scheme requires $|\lambda_{cx}| \leq 2$, and for advection alone, $|\lambda_u| \leq 2$. Thus, for acoustic modes coupled with advection, it is the sum of the parameters that determines the stability limit.

The dispersion relations for the continuous equations (19) and (20) and for the discrete system (21) and (22) with $n_s = 1$ are

$$\omega\Delta t = \frac{1}{2}(\lambda_u \pm \lambda_{cx}) = k(U \pm c)\Delta t$$

and

$$\omega\Delta t = \sin^{-1}\left[\frac{1}{2}(\lambda_u \pm \lambda_{cx})\right],$$

respectively. As is well known, the leapfrog scheme has no amplitude error (ω is always real) and has a positive phase error, that is, as $\omega\Delta t$ (exact) approaches ± 1, the dimensionless phase in the scheme approaches $\pm\pi/2$.

The amplification factors for the scheme are given by $A = \exp[\mathrm{Im}(\omega\Delta t)]$, using $\omega\Delta t$ from the dispersion relation for the discretized system. Figure 1a shows a plot of the maximum amplification factor for the non-time-split scheme ($2\Delta t = \Delta\tau$; i.e., $n_s = 1$) as a function of λ_u and λ_{cx}. The line AB in Fig. 1a represents the modes that will be present in a linear computation with an example value of $U/c_s = 1/12$. The slope of AB is $\lambda_u/\lambda_{cx} = 2U\Delta t/c_s\Delta\tau$ and in Fig. 1 $U/c_s = 1/12$. Typically, $c_s \gg U$, so the slope of AB will be small for a single small time step per large time step ($2\Delta t = \Delta\tau$), and the maximum allowable large time step will result in a Courant number ($Uk\Delta t = \lambda_u/2$) of much less than 1. In elastic models, the cost of evaluating all the non-acoustic terms on the large time step such as advection, mixing, etc. is much greater than the small-time-step calculations, and the advantage of the KW time-split scheme is that larger large time steps can be taken by using several small time steps per large time step. In most models, it is computationally more efficient to have a slope for AB that is order 1. The KW time-split scheme raises the slope of AB by decreasing $\Delta\tau$, that is, taking more small time steps for a given large time step. As can be observed in Figs. 1a–d, the slope of AB increases with increasing n_s for a fixed U/c_s. In practice, the large time step is specified such that the Courant condition for advection is 0.5 or less, so as to keep phase errors within reasonable bounds. Having chosen a large time step, the number of small time steps is chosen such that the Courant condition on the hori-

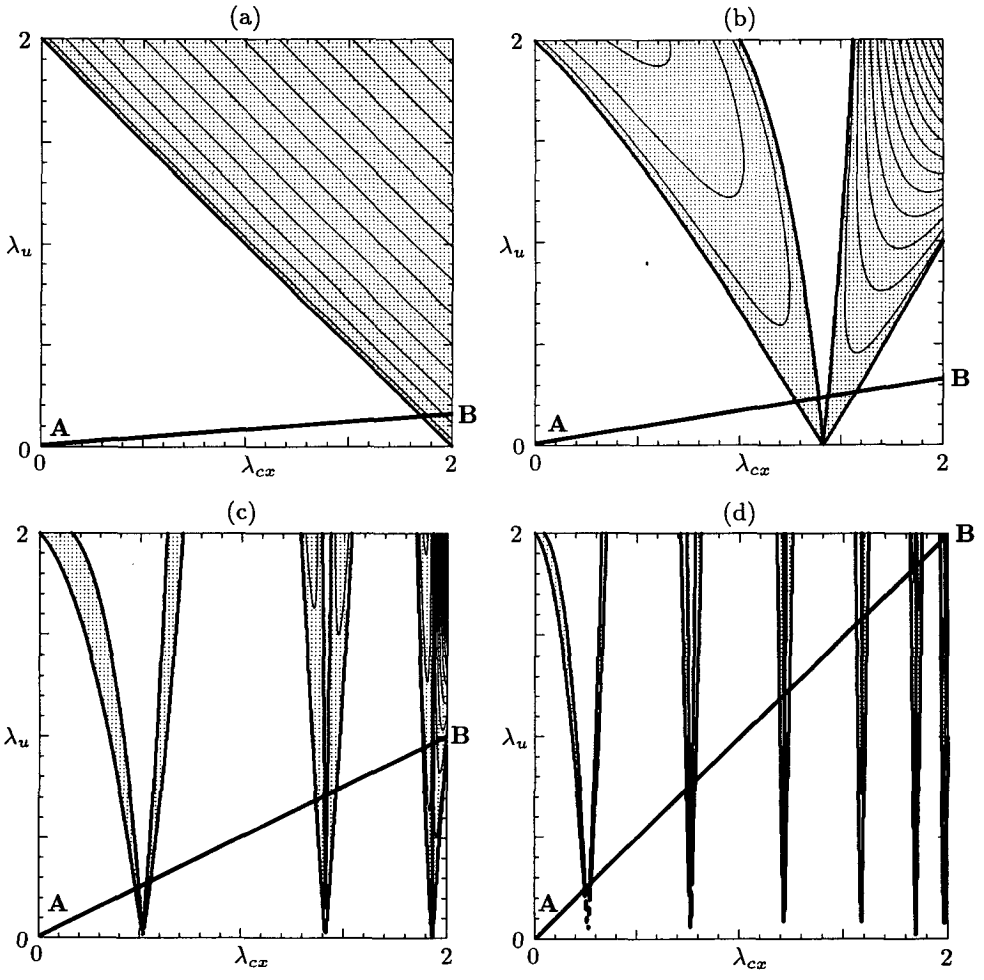

FIG. 1. (a) Amplification factor for the explicit acoustic-advection system with one small time step per large time step. The thick line is the 1.0 contour and the minor contours are at intervals of 0.2. The stippled region denotes an amplification factor greater than 1. (b) As in (a) with $n_s = 2$, (c) $n_s = 6$, and (d) $n_s = 12$. The lines AB are plotted using $U/c_s = 1/12$.

zontally propagating sound waves is close to 1. The only concern with the acoustic integrations is stability, not accuracy, hence the high Courant number for the acoustic modes.

Note that in nonlinear computations, possible modes lie along and below (to the right of) the line AB and not above (to the left of) AB, because U will vary, being bounded by some $U_{\max}$, but c_s will always be large, and in some models a constant sound speed is used (Droegemeier and Wilhelmson 1987). Hence, we must have stability below and to the right of AB.

The stability diagram in Fig. 1a holds only for a single small time step per large time step. The stability space for $n_s > 1$ must be examined to determine whether anything is gained by increasing n_s. For an even number of small time steps per large time step, the characteristic equation for the dispersion relation for the discrete system is

$$(B_m^2 - \lambda_{cx}^2 B_m + \lambda_{cx}^2)\sin^2(\omega\Delta t) - \lambda_u^2\left(B_m - \frac{\lambda_{cx}^2}{2}\right) \times \sin(\omega\Delta t) - \left(\lambda_{cx}^2 - \frac{\lambda_u^2}{4}\right)\left(1 - \frac{\lambda_{cx}^2}{4}\right) = 0, \quad (23)$$

where

$$B_m = \frac{B_{m-1} - \lambda_{cx}^2}{1 + B_{m-1} - \lambda_{cx}^2},$$

$B_1 = 1$ and $m = n_s/2$. Equation (23) is derived by taking n_s small time steps with (21) and (22), eliminating variables at times other than t, $t - \Delta t$, and $t + \Delta t$, and finally using a Fourier representation in time. Figures 1b, 1c, and 1d show plots of the amplification factor for $n_s = 2$, 6, and 12, respectively. The usable stable region in these diagrams is that directly to the right and above the origin. The instabilities depicted in these figures were first discovered by Tatsumi (1983) in his von Neumann analysis of the 1D system for his use of the KW scheme in a hydrostatic model. It is immediately obvious that these instabilities cause the usable stable region for the scheme to shrink dramatically as more small time steps are taken, although the amplification in unstable regions also decreases significantly.

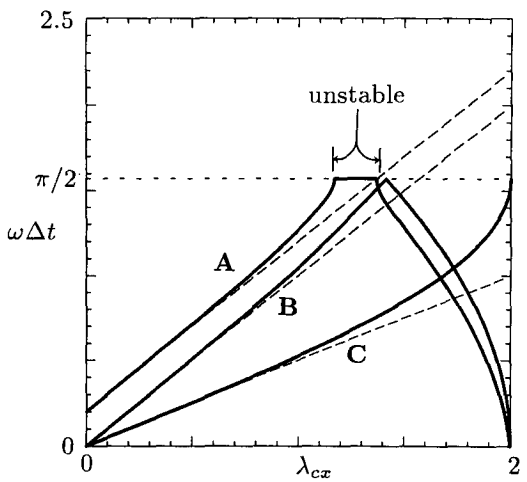

FIG. 2. Dimensionless frequency for the time-split system with explicit integration of the acoustic modes, for $\omega\Delta t$ as a function of λ_{cx} with (a) $n_s = 2$, $\lambda_u = 0.4$, (b) $n_s = 2$, $\lambda_u = 0$, and (c) $n_s = 1$, $\lambda_u = 0$. The exact frequencies are illustrated with dashed lines.

The source of the instability responsible for the shrinking stable region can be appreciated by closer examination of the dispersion relation (23). With $n_s = 2$, the solution for $\sin(\omega\Delta t)$ in (23) is

$$\sin(\omega\Delta t) = \frac{1}{2}\lambda_u\left(1 - \frac{\lambda_{cx}^2}{2}\right) \pm \left[\frac{\lambda_u^2}{4}\left(1 - \frac{\lambda_{cx}^2}{2}\right)^2 + \left(\lambda_{cx}^2 - \frac{\lambda_u^2}{4}\right)\left(1 - \frac{\lambda_{cx}^2}{4}\right)\right]^{1/2}. \quad (24)$$

Consider first the dispersion relation with no advection ($\lambda_u = 0$):

$$\sin(\omega\Delta t) = \pm\lambda_{cx}\left(1 - \frac{\lambda_{cx}^2}{4}\right)^{1/2}. \quad (25)$$

Figure 2 is a plot of $\omega\Delta t$ versus λ_{cx} with n_s equal to 1 and 2; $\omega\Delta t$ is the dimensionless frequency as *observed* on the large time step. For a given Δt, the highest acoustic frequency that can be present on the small time step when n_s equals 2 is double that present when n_s equals 1 (compare the exact frequencies in Fig. 2). For n_s equal to 1, there are no frequencies greater than $\pi/2$ in the stable regime; however, for n_s greater than one, higher frequencies exist on the small time step in the stable regime and these higher frequencies are aliased. Thus, while the single small-time-step scheme becomes unstable after $\omega\Delta t = \pi/2$ (period of $4\Delta t$, $\lambda_{cx} = 2$), the scheme with two small time steps becomes unstable after the frequency returns to zero and becomes complex [see (25)]. Critically important is the fact that the large time step sees $4\Delta t$ modes for $\lambda_{cx} < 2$, and for $n_s = 2$, this occurs at $\lambda_{cx} = \sqrt{2}$ [see (25)].

Next, consider the addition of advection on the large time step. Examination of Fig. 1b reveals that two unstable modes, centered about $\lambda_{cx} = \sqrt{2}$, arise with the addition of advection. The instabilities derive from the advection of the two acoustic modes ($\omega\Delta t \approx \pm\pi/2$) that appear as high frequencies on the large time step over which the advection is calculated. Figure 2 includes a plot of $\omega\Delta t$ showing the positive root of (24) for $n_s = 2$ with $\lambda_u = 0.4$ (the instability to the left of $\lambda_{cx} = \sqrt{2}$ in Fig. 1b). The instability is apparent and is clearly linked to the $\omega\Delta t = \pi/2$ acoustic mode. The instability to the right of $\lambda_{cx} = \sqrt{2}$ in Fig. 1b is associated with the advection of the $-\pi/2$ acoustic mode.

Closer examination of Figs. 1a–d reveals several more characteristics of the instability. First, the size of the stable region shrinks with an increasing number of small time steps. Second, the amplitude of the instability first encountered when moving from left to right in the stability diagrams in Fig. 1 decreases with increasing n_s. Next, the width of the instability and its maximum amplitude increase with increasing λ_u. Finally, the number of $\pm\pi/2$ aliased modes increases with increasing n_s, and the actual number of $\pm\pi/2$ aliased modes is $n_s/2$.

It is the first instability (aliased acoustic mode) encountered as λ_{cx} is increased that is important because this boundary will determine the maximum large and small time steps that can be taken. The line AB in Fig. 1c has a slope six times that of AB in Fig. 1a, representing a computation identical to AB in Fig. 1, except that six small time steps are now taken per large time step. Unfortunately, the maximum allowable large time step is not six times as large for $n_s = 6$ as compared with $n_s = 1$; hence, taking more small time steps does not significantly decrease computational costs. Indeed, the actual computational cost may increase.

The stability analysis suggests that the KW scheme should not increase efficiency when more small time steps are taken; the stable region shrinks and the large time step cannot be increased appreciably. However, this instability has not hampered the use of this KW time-split scheme because the instability manifests itself as short-period modes on the large time step ($4\Delta t$) and these modes are efficiently damped by a Robert time filter (Robert 1966; Asselin 1972). Figure 3 shows the maximum amplification factor along the line AB as a function of α for the case $n_s = 6$. These results were produced using the von Neumann analysis described in the Appendix. Even for small values of the Robert filter coefficient α, the unstable modes are stabilized

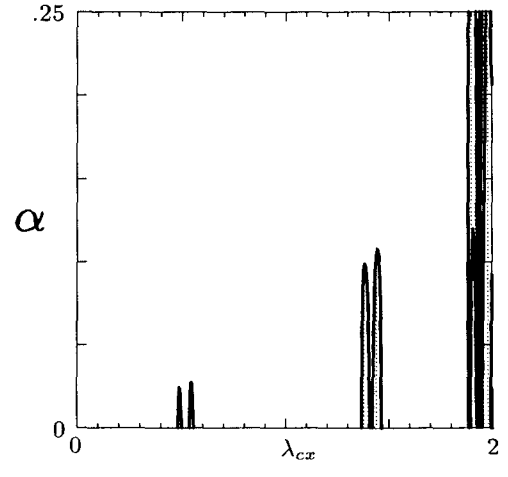

FIG. 3. Amplification factor for integration of the modes on line AB in Fig. 1c, where $\lambda_u = \lambda_{cx}/2$, versus the Robert filter coefficient α. Contouring is as in Fig. 1.

and the scheme can be run close to the limiting Courant conditions for the *individual* large- and small-time-step schemes. Thus, while the Robert time filter is used to prevent temporal decoupling of the solution in the large-time-step leapfrog scheme, it also serves to stabilize the explicit time-split method of KW and masks the fact that the stability of the individual small- and large-time-step schemes does not ensure the stability of the coupled system. Tatsumi also recognized that the Robert filter effectively damps these instabilities, though he does not show that the instabilities are related to the advection of high-frequency acoustic modes.

b. *Stability analysis with implicit differencing*

By treating the vertically propagating sound waves implicitly, the large and small time steps do not interact in the same manner as their horizontal counterparts. The discrete equations for this case are (17) and (18), with $\lambda_u = 0$, $\lambda_{cx} = 0$, and $\lambda_N = 0$. In the linearized equations (1)–(4) the mean vertical velocity is assumed to be zero. In nonlinear computations, there will be regions of significant vertical advection that can have an impact on the stability of the overall numerical scheme. Hence, we add a mean vertical advection and (17) and (18) become

$$w^{\tau+\Delta\tau} = w^{\tau} - \frac{i\lambda_{cz}}{2}(p^{\tau+\Delta\tau} + p^{\tau}) - \frac{i}{n_s}\lambda_w w^{t}, \quad (26)$$

$$p^{\tau+\Delta\tau} = p^{\tau} - \frac{i\lambda_{cz}}{2}(w^{\tau+\Delta\tau} + w^{\tau}) - \frac{i}{n_s}\lambda_w p^{t}, \quad (27)$$

where $\lambda_w = 2\Delta t/W$. For $n_s = 1$, this system is equivalent to the semi-implicit approximation analyzed by Kwizak and Robert (1971). They have shown that the discretization

$$\phi^{n+1} = \phi^{n-1} - i\lambda_w\phi^{n} - \frac{i\lambda_{cz}}{2}(\phi^{n+1} + \phi^{n-1})$$

is stable whenever $\lambda_w^2 \leq 1 + \lambda_{cz}^2$. We have verified that this result remains valid for the system (26) and (27), and the von Neumann analysis shows that the stability criteria become even less restrictive as n_s increases, in contrast to the horizontal case.

Increasing the number of small time steps per large time step does not destabilize the implicit acoustic-mode–explicit advection system. Figure 4 shows the frequency $\omega\Delta t$ for the implicit acoustic integrations for $n_s = 2$ and can be compared to the explicit scheme results for $n_s = 2$ in Fig. 2. The large time step does see aliased $\omega\Delta t = \pm\pi/2$ modes much as in the horizontal case. However, the addition of advection does not destabilize the scheme; the advection of high-frequency acoustic modes is stable.

The strong stability of this leapfrog-based semi-implicit scheme has been taken advantage of in many nonhydrostatic models, for example, the United King-

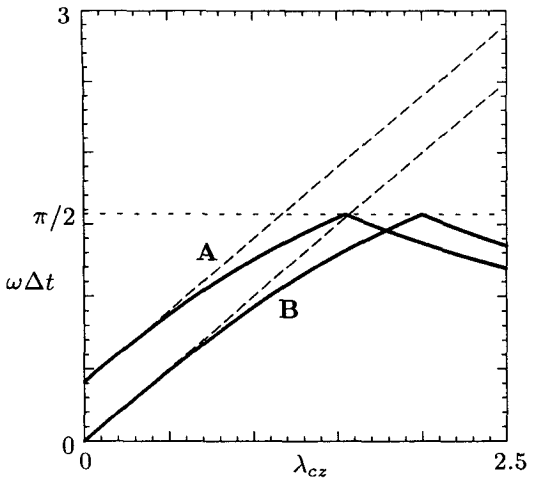

FIG. 4. Dimensionless frequency $\omega\Delta t$ as a function of λ_{cz} with $n_s = 2$ and (a) $\lambda_u = 0.4$ and (b) $\lambda_u = 0$. The exact frequencies are illustrated with dashed lines.

dom Meteorological Office model (Golding 1987; Cullen 1990), Tanguay et al. 1990, and others, and it forms the numerical basis of many hydrostatic models.

c. An acoustic-mode filter

Acoustic modes in nonlinear models are easily excited by model physics, boundary conditions, nonlinear processes, etc., and in general it is beneficial to filter these modes. The Robert filter does not damp acoustic modes directly, since it operates on the large time step. In order to provide some filtering of the acoustic modes, DK introduced the off-centered time differencing for the implicit terms in the vertical momentum equation and pressure equation. Equations (26) and (27), with the off-centering parameter included, become

$$w^{\tau+\Delta\tau} = \omega^{\tau} - i\lambda_{cz}\left(\frac{1+\beta}{2}\,p^{\tau+\Delta\tau} + \frac{1-\beta}{2}\,p^{\tau}\right)\frac{i}{n_s}\,\lambda_w w^t, \tag{28}$$

$$p^{\tau+\Delta\tau} = p^{\tau} - i\lambda_{cz}\left(\frac{1+\beta}{2}\,w^{\tau+\Delta\tau} + \frac{1-\beta}{2}\,w^{\tau}\right) - \frac{i}{n_s}\,\lambda_w p^t. \tag{29}$$

Using $\beta > 0$ preferentially damps high-frequency modes that have vertical structure, although it does not damp horizontally propagating modes with vertical wavenumber 0. A filter for horizontally propagating sound waves has been proposed by Ikawa (1988), where (22) is replaced by

$$p^{\tau+\Delta\tau} = p^{\tau} - i\lambda_{cx}\left(\frac{1+\gamma}{2}\,u^{\tau+\Delta\tau} + \frac{1-\gamma}{2}\,u^{\tau}\right) - \frac{i}{n_s}\,\lambda_u p^t.$$

The KW scheme is recovered by using $\gamma = 1$. Ikawa suggests the use of $\gamma > 1$ to filter horizontally propagating sound waves and $\beta = 1$ to filter vertically propagating sound waves along with Robert time filtering. Von Neumann analyses confirm that using $\gamma > 1$ will further stabilize the time-split scheme because it damps all horizontally propagating modes.

We believe that filtering the acoustic modes by using $\beta > 0$ and $\gamma > 1$ can be detrimental to the solution, because these filters provide at least some damping of all propagating waves with horizontal or vertical structure. Therefore, a new acoustic filter has been constructed based on the characteristic that only the acoustic modes have nonzero divergence. Divergent modes can be selectively damped by including an additional term in the momentum equations. Ignoring advection, the new system is

$$u_t + c_s p_x - \alpha_d D_x = 0, \tag{30}$$

$$w_t + c_s p_z - N\theta - \alpha_d D_z = 0, \tag{31}$$

$$\theta_t + Nw = 0, \tag{32}$$

$$p_t + c_s D = 0, \tag{33}$$

where $D = u_x + w_z$. The addition of the terms involving the divergence in (30) and (31), with a suitable choice of α_d, is an effective filter for acoustic modes. This can be demonstrated by forming an equation for the divergence from (30) and (31):

$$D_t + c_s^2\nabla^2 p - N\theta_z = \alpha_d\nabla^2 D.$$

The inclusion of the new terms serves to diffuse the divergence, thus filtering the sound waves. Divergence damping is applied on the small time steps in the KW scheme. The divergence terms are evaluated at time level τ in the small-time-step system and, as expected with an explicit evaluation of a ∇^2-type dissipation term, stability requires that $\alpha_d\Delta\tau/\Delta x^2 \leq 1/2$.

The divergence damping does not appreciably damp any other modes in the system. Intuitively, we would expect this because the anelastic equations, which explicitly require that the divergence be zero, are successfully used for atmospheric simulations. The dispersion relation for the linear system (30)–(33) with the divergence damping terms included is

$$\omega^4 + i\alpha_d(k^2+l^2)\omega^3 - [c_s^2(k^2+l^2) + N^2]\omega^2 - i\alpha_d k^2N^2\omega + c_s^2k^2N^2 = 0. \tag{34}$$

While the damping properties of the scheme are not obvious in (34), we can surmise that the new terms should have little effect on the gravity waves because the terms involving α_d cancel when the anelastic gravity-wave frequency $\omega^2 = k^2N^2/(k^2+l^2)$ is substituted into (34). By nondimensionalizing (34) with the zero-order acoustic frequency $\omega_0^4 = c_s^4(k^2+l^2)^2$ and defining a small parameter $\epsilon = \alpha_d(k^2+l^2)^{1/2}/c_s$, the dispersion relation (34) can be written as

$$\tilde{\omega}^4 + i\epsilon\tilde{\omega}^3 - (1 + \tilde{N}^2)\tilde{\omega}^2 - i\epsilon\tilde{N}^2(1 - \tilde{l}^2)\tilde{\omega} + \tilde{N}^2(1 - \tilde{l}^2) = 0,$$

where $\tilde{\omega} = \omega/\omega_0$ is the dimensionless frequency, $\tilde{N}^2 = N^2/[c_s^2(k^2 + l^2)]$, and $(1 - \tilde{l}^2) = k^2/(k^2 + l^2)$. Representing $\tilde{\omega}$ as an expansion in the small parameter ϵ, $\tilde{\omega} = \tilde{\omega}_0 + \epsilon\tilde{\omega}_1 + \epsilon^2\tilde{\omega}_2 + \cdots$, we can solve for the corrections to the solution of the original system $\tilde{\omega}_0$. The first-order correction is

$$\tilde{\omega}_1 = i\tilde{\omega}_0 \frac{\tilde{n}^2(1 - \tilde{l}^2) - \tilde{\omega}_0^2}{4\tilde{\omega}_0^3 - 2\tilde{\omega}_0(1 - \tilde{n}^2)}.$$

Figure 5 shows the first correction term $\tilde{\omega}_1$ relative to $\tilde{\omega}_0$ (i.e., $\tilde{\omega}_1/\tilde{\omega}_0$) for the gravity-wave frequency. This imaginary component of the frequency results in damping of the waves, and over a single wave period a wave will be damped $\exp[2\pi\epsilon(\tilde{\omega}_1/\tilde{\omega}_0)]$. This damping is negligible. The next-order correction has been calculated and is significantly smaller then the leading-order correction term.

This acoustic filter also stabilizes the explicit acoustic-advection system. For example, the damping provided by the use of a Robert filter coefficient of 0.2 in Fig. 3 is approximately equaled by using a dimensionless divergence damping coefficient $\alpha_d c_s^{-2}\Delta\tau^{-1} = 0.1$. Divergence damping is a viable alternative to Robert time filtering for stabilizing the explicit acoustic mode–advection instability.

Our linear stability analyses have been verified with nonlinear integrations of the nonlinear version of (1)–(4). Moreover, in integrations where we include the divergence damping, and where there is no mean stability, we have produced stable integrations without the use of the Robert time filter. Divergence damping does not prevent decoupling of time levels often observed in leapfrog integrations, so Robert filtering is still needed in most calculations; however, the results of integrations using divergence damping increases our confidence in using a small Robert coefficient. In cloud models, the typical value of α is 0.1–0.2. Now $\alpha = 0.05$ or less is used. Also, the divergence term must be differenced in a manner that would produce the correct discretized divergence equation and pressure equation as derived from the discretized momentum equations and pressure equation, that is, the discretization of the divergences and pressure gradients must be consistent.

Finally, we note that the concept of filtering the divergence is not entirely new. Hydrostatic primitive equation models have made use of similar terms in the *horizontal* momentum equation where the divergence of the *horizontal* wind field is diffused. This damps internal and inertial gravity waves. The approach was first presented by Morel and Talagrand (1974) in the context of data assimilation. It has since been used in models by Sadourny (1975), Bates and McDonald (1982), and others. It is stressed that our application uses the divergence of the full wind field and leaves gravity waves essentially unaffected. Also, artificial compressibility methods for solving the incompressible, steady-state Navier–Stokes equations also make use of divergence damping (Ramshaw and Mousseau 1990).

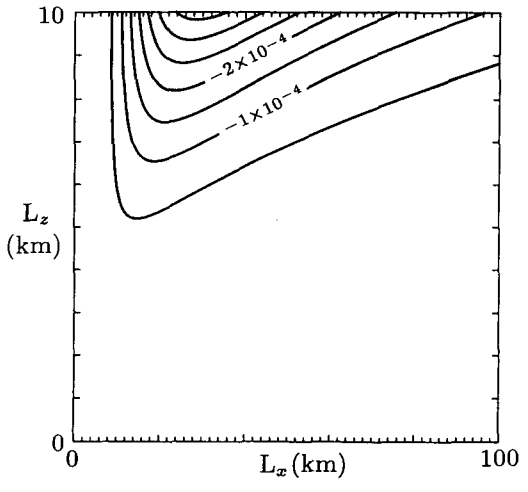

FIG. 5. Correction term $\tilde{\omega}_1/\tilde{\omega}_0$ divided by i.

d. *Stability of the gravity-wave modes*

In the KW time-split scheme, the interactions between propagating and advecting components of sound and gravity waves also lead to instabilities similar to, though generally weaker than, those arising from the interaction of horizontally propagating and advecting portions of acoustic modes. These instabilities are not present in the non–time-split system.

For (15)–(18), with $n_s = 1$, the dispersion relation is

$$\left(\sin\omega\Delta t - \frac{\lambda_u}{2}\right)^2 = \frac{(\lambda_{cx}^2 + \lambda_{cz}^2 + \lambda_N^2)}{8(1 + \lambda_{cz}^2/4)} \times \left\{1 \pm \left[1 - \frac{4\lambda_{cx}^2\lambda_N^2(1 + \lambda_{cz}^2/4)}{(\lambda_{cx}^2 + \lambda_{cz}^2 + \lambda_N^2)^2}\right]^{1/2}\right\}. \quad (35)$$

Disregarding advection and acoustic modes, the stability requirement for the buoyancy calculations is $\lambda_N < 2$. Stability of the acoustic–gravity-wave scheme requires that the right-hand side of Eq. (35) be less than or equal to one. The stability requirement from (35) is, surprisingly,

$$\lambda_{cx}^2, \lambda_N^2 \leq 4, \quad (36)$$

and is not $\lambda_{cx}^2 + \lambda_N^2 \leq 4$ as might be expected. Here λ_{cz} only serves to change the amplitude of the instabilities, and as $\lambda_{cz} \to \infty$ the scheme is unconditionally stable.

A von Neumann analysis of the KW system (15)–(18), for $n_s > 1$, reveals weak instabilities for $\lambda_N \leq 2$. Figure 6 depicts the stability space for the scheme as a function of λ_{cx}, λ_{cz}, and λ_N. The instabilities reported

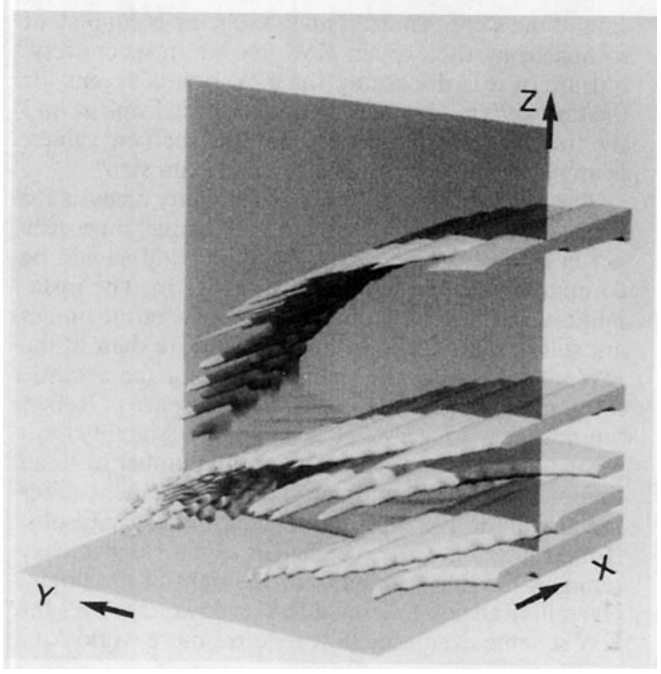

FIG. 6. Amplification factor for the acoustic–gravity-wave system. On the x axis $0 \leq \lambda_N \leq 3$, on the y axis $0 \leq \lambda_{cx} \leq 2$, and on the z axis $0 \leq \lambda_{cz} \leq 10$. The y–z plane lies at $\lambda_N = 2$. The region where $|A| \geq 1.0$ is enclosed by the contour surfaces. Note the instabilities found in the region $\lambda_N < 2$.

by DK, which were remedied by off centering the semi-implicit part of the small time step [$\beta > 0$ in (28) and (29)], likely are the instabilities shown in Fig. 6. Filtering the acoustic modes with the divergence damping effectively removes the instabilities for $\lambda_N \leq 2$, and use of a nonzero β is no longer necessary, even in case of large atmospheric stability.

For large atmospheric stability, that is, when a stratosphere is included in the domain, Δt is increasingly limited by the buoyancy (λ_N) as Δx grows large (wavenumber k grows small). In simulations where Δx is only a few kilometers, the atmospheric stability has little effect on the allowable time step, but when Δx grows larger than 10–20 km, the time-step limitation can become significant. This is apparent in (35), where the term multiplying the term in the large brackets represents the acoustic mode. As k decreases and Δt increases, the stability condition $\lambda_N^2 \leq 4$ becomes more restrictive than $\lambda_{cx}^2 \leq 4$ because the stability starts contributing appreciably to the acoustic-mode frequency. While the stability criterion (36) is for $n_s = 1$, the limit is not appreciably altered by increasing n_s for large Δt.

We are employing nonhydrostatic models on the mesoscale and the synoptic scale (Snyder et al. 1991), and have encountered this time-step restriction. To circumvent the restriction, we employ a technique where the vertical advection of θ and the buoyancy term in the vertical momentum equation are computed implicitly on the small time step.

The discretized equations replacing (15) and (17) are

$$\theta^{\tau+\Delta\tau} = \theta^{\tau} - \frac{\lambda_N^*}{2}(w^{\tau+\Delta\tau} + w^{\tau}) - i\lambda_u\theta^t, \quad (37)$$

and

$$w^{\tau+\Delta\tau} = w^{\tau} - \frac{i\lambda_{cz}}{2}(p^{\tau+\Delta\tau} + p^{\tau}) - \frac{i}{n_s}\lambda_u w^t + \frac{\lambda_N^*}{2}(\theta^{\tau+\Delta\tau} + \theta^{\tau}), \quad (38)$$

where $\lambda_N^* = \lambda_N/n_s$, and the divergence-damping term presented in (31) has been omitted. In the dispersion relation for the linear system (16), (18), (37), and (38), the $1 + \lambda_z^2/4$ term in the denominator of the first term in (35) becomes $1 + \lambda_z^2/4 + \lambda_N^{*2}/4$. Hence, the stability limitation associated with λ_N is removed. Von Neumann analyses show that this result is valid for any number of small time steps per large time step. Also, θ can be computed explicitly on the small time step with a stability restriction of $\lambda_N^* \leq 2$.

The addition of the implicit interdependence of θ and w does not complicate the small-time-step solution procedure. As in the original KW system, only a one-dimensional Helmholtz equation needs to be solved; θ is advanced in a manner analogous to p on the small time step. In the full nonlinear model, the term analogous to the linear term Nw in (3) will be the nonlinear term $w(x, y, z, t)\partial\theta(x, y, z, t)/\partial z$. The new term must be linear if it is to be computed implicitly on the small time step. This is accomplished by vertically advecting the perturbation potential temperature on the large time step, $w^t\partial[\theta - \bar{\theta}(z)]/\partial z$, and advecting the time-independent mean on the small time step, $\frac{1}{2}(w^{\tau} + w^{\tau+\Delta\tau})\partial\bar{\theta}(z)/\partial z$. We have compared three versions of the scheme, the first with buoyancy calculations completely on the large time step (the traditional KW scheme), the second with the vertical advection of buoyancy and the evaluation of the buoyancy term in the vertical momentum calculation performed explicitly on the small time step, and the third being the scheme described by (37) and (38). In all cases, no discernible differences in the solutions have been found. This observation holds even when the mean buoyancy profile $\bar{\theta}(z)$ does not represent the buoyancy profile in an individual column well, as in the case with a sloping tropopause. In semi-implicit hydrostatic models, the choice of a reference temperature profile about which to linearize the vertical advection of buoyancy appears to be more critical. This is analyzed in detail in Simmons et al. (1978).

The general approach of integrating the terms responsible for gravity waves in the same manner as the acoustic terms was introduced simultaneously by Cul-

len (1990) and by Tanguay (1990) in semi-implicit nonhydrostatic models. An extension of the technique to the explicit time-split scheme of KW has been presented.

5. Alternative schemes

The KW time-split scheme appears to be the best available explicit time-split method for integrating the hydrostatic and nonhydrostatic systems based on its stability and simplicity. However, there are two major reasons for seeking an alternative scheme. The Robert-filtered leapfrog scheme is not second-order accurate in time (see Durran 1991) and higher time accuracy is desirable, particularly when using highly accurate spatial discretizations. The leapfrog scheme is also somewhat inefficient in that the acoustic modes must be integrated from $t - \Delta t$ to $t + \Delta t$ for each time step. Schemes that would allow integrations from only t to $t + \Delta t$ halve the computations required to integrate the acoustic modes.

The interaction between acoustic modes and advection has the greatest impact on the stability of the time-split schemes, hence, several advection schemes will be examined for the linear momentum equations (5) and (6) with the acoustic modes integrated using the small-time-step scheme given in (16)–(18). Examples from two classes of schemes will be considered: pure time-integration schemes in which the spatial discretization need not be considered and forward-in-time schemes for advection where the spatial discretization and flow direction must be included in the analyses.

Before examining new schemes, we consider a scheme that is very similar to the KW splitting scheme and that is commonly used in hydrostatic models.

a. *Madala's scheme for hydrostatic models*

Madala (1981) presents a scheme for use in a hydrostatic model. Using the notation in section 4, integration of the acoustic-advection system (or the analogous shallow-water system) with Madala's scheme can be examined using the following difference equations:

$$u^{t+\Delta t} = u^{t-\Delta t} - i\lambda_{cx}\bar{p}^{t} - \lambda_u u^{t},$$

$$p^{t+\Delta t} = p^{t-\Delta t} - i\lambda_{cx}\bar{u}^{t} - \lambda_u p^{t},$$

where the operator $\bar{\phi}^t$ is defined as

$$\bar{\phi}^{t} = \frac{1}{2\Delta t}\int_{t-\Delta t}^{t+\Delta t} \phi dt.$$

This scheme is equivalent to using a leapfrog scheme for all modes, except that the pressure gradient and divergence terms are differenced using time-averaged values. To obtain these time-averaged values, Madala integrates the small-time-step equations similar to (21) and (22) used in KW and averages the results over the small time steps. Thus, Madala's scheme is equivalent to first using the explicit KW scheme in its entirety, but afterwards discarding the KW results except for the time-averaged values, and then using leapfrog and the time-averaged values to compute the new values. Is anything gained by including this extra step?

The results of a von Neumann stability analysis for the Madala scheme where there are six small time steps per large time step are given in Fig. 7 and should be compared with the KW results in Fig. 1c. The instabilities associated with the advection of acoustic modes are still present and they are more severe than in the KW scheme. Also, the stability limit for the acoustic integration without advection, in the absence of Robert filtering, is no longer $\lambda_{cx} \leq 2$, which is the stability limit for the KW scheme regardless of the number of small time steps per large time step. The loss of stability arises because of the averaging of the small-time-step results. Robert filtering with a coefficient $\alpha = 0.15$ effectively removes the first instability to the right of the origin. Overall, Madala's scheme offers no advantage over the KW scheme even though it requires more work.

b. *Pure time-integration schemes*

There are few alternate time-integration schemes that might be attractive alternatives to leapfrog. The largest cost in a model time step is that arising from the evaluation of the large-time-step terms, that is, advection, mixing, model physics, etc. In order that the model be economical, only a single evaluation of these terms per time step is desirable. Also, schemes that require multiple evaluations may be difficult to time split in a straightforward manner. For example, it is not clear how one would use a fourth-order Runge–Kutta

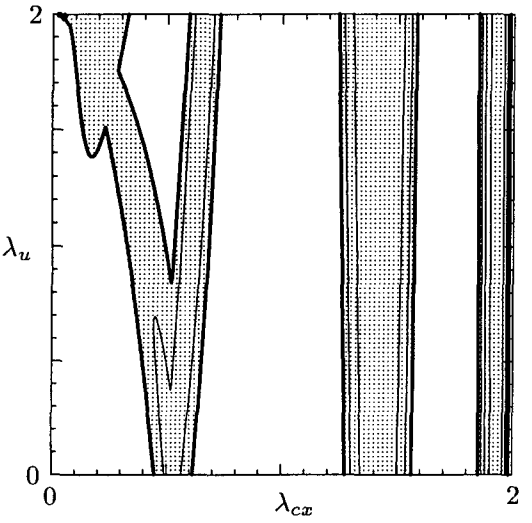

FIG. 7. Amplification factor for the explicit acoustic-advection system with the Madala (1981) scheme. There are six small time steps per large time step. Contours are as in Fig. 1.

scheme for evaluating the advection terms in a time-split model.

One possible scheme for evaluating the large-time-step advection terms is the third-order Adams–Bashforth scheme (AB3) recently reexamined by Durran (1991). For the equation

$$\frac{d\phi}{dt} = F(\phi) \tag{39}$$

the AB3 time integration scheme is

$$\phi^{t+\Delta t} - \phi^t = \frac{\Delta t}{12}[23F(\phi^t) - 16F(\phi^{t-\Delta t}) + 5F(\phi^{t-2\Delta t})].$$

Only the term $F(\phi^t)$ needs to be computed for the time step, the other evaluations of F have been computed and stored in the two previous time steps.

For horizontally propagating and advecting acoustic modes, the discretized system is

$$u^{\tau+\Delta\tau} = u^\tau - i\lambda_{cx}p^\tau - \frac{i\lambda_u}{12n_s}(23u^t - 16u^{t-\Delta t} + 5u^{t-2\Delta t}),$$

$$p^{\tau+\Delta\tau} = p^\tau - i\lambda_{cx}u^{\tau+\Delta\tau} - \frac{i\lambda_u}{12n_s}(23p^t - 16p^{t-\Delta t} + 5p^{t-2\Delta t}).$$

In this scheme, $n_s = \Delta t/\Delta\tau$ small time steps are taken, marching from time t to time $t + \Delta t$. In this case, $\lambda_u = \Delta tkU$ as opposed to $\lambda_u = 2\Delta tkU$ in the leapfrog analysis. The results of von Neumann analyses of the scheme are given in Fig. 8. Instabilities similar to those found with the leapfrog time-split scheme are present.

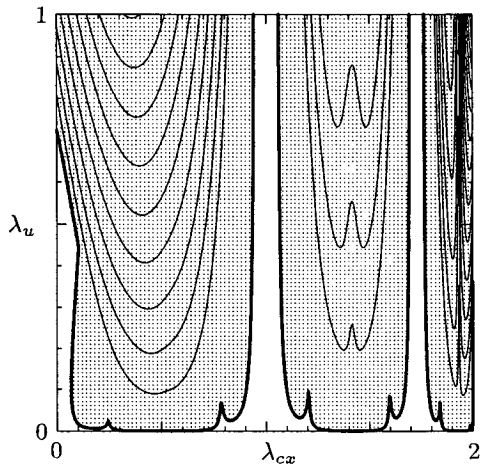

FIG. 8. Amplification factor for the explicit acoustic-advection system with the third-order Adams–Bashforth scheme used for advection. There are six small time steps per large time step. Contouring is as in Fig. 1.

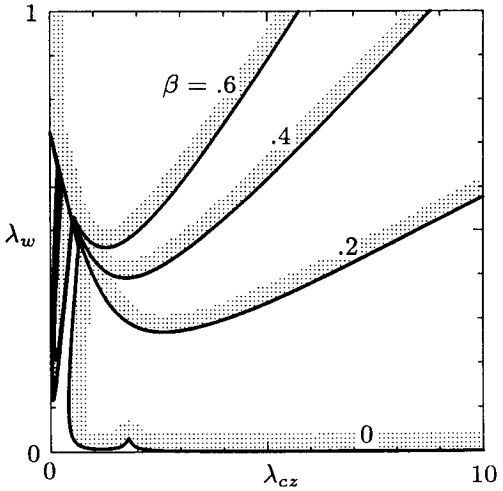

FIG. 9. Amplification factor for the implicit acoustic-advection system with the third-order Adams–Bashforth scheme used for advection. There is only one small time step per large time step and results are shown for both a centered and off-centered implicit scheme where β = 0, 0.2, 0.4, and 0.6. The contours are at 1.0 and the stippling denotes the side of the contours where the amplification factor is greater than 1. The instabilities that appear adjacent to the λ_w axis for increasing values of β are not for modes present in most calculations.

However, the strength of the instabilities are much larger than in the leapfrog scheme (cf., Fig. 1d), and explicit small time steps are not feasible with the AB3 scheme, even with divergence damping.

Durran has analyzed the semi-implicit scheme given in (26) and (27) for the case where the advection terms are evaluated using AB3 and where the small time step is equivalent to the large time step. The results for the von Neumann analysis are given in Fig. 9. Off centering the implicit calculations, that is, $\beta > 0$ in (28), will damp the instabilities. However, the acoustic computations would need to be implicit in all spatial directions, and a multidimensional Helmholtz equation would need to be solved.

Durran (1991) also briefly discusses other time-stepping schemes, one of which is the second-order Magazenkov method (Magazenkov 1980). The method consists of alternating leapfrog time steps with second-order Adams–Bashforth (AB2) time steps. The AB2 scheme for integrating (39) is

$$\phi^{t+\Delta t} - \phi^t = \frac{\Delta t}{2}[3F(\phi^t) - F(\phi^{t-\Delta t})].$$

Again, only one function evaluation per time step is needed. As a time-stepping scheme where $F(\phi) = i\lambda_u$, AB2 is unconditionally unstable. However, the instabilities are weak for small Courant numbers and several modelers have employed the scheme for short-time integrations with viscosity (Deardorff 1974; Moeng 1984).

Interestingly, Magazenkov's combination of the neutral scheme and the unconditionally unstable scheme produces a stable scheme that damps slightly. The Magazenkov scheme allows a maximum Courant number of 0.71 for pure advection. The stability diagram for the Magazenkov scheme used in a time-split system where the acoustic modes are integrated explicitly on a small time step with $n_s = 6$ is given in Fig. 10. The instabilities associated with the advection of high-frequency acoustic modes appear but are much weaker than in the AB3 scheme. Nonlinear calculations with the scheme reveal that these are sufficiently damped by divergence damping. The limiting Courant conditions for the time-split system are essentially the limiting conditions for the individual small- and large-time-step scheme. Implicit integrations for the vertically propagating acoustic modes reveal no added instabilities that are not sufficiently damped by the divergence damping. Thus, the Magazenkov scheme appears to be a reasonable alternative to the leapfrog scheme for the large-time-step calculations. Its only drawback is the increased coding complexity involved in alternating schemes every time step, which may be significant in large codes.

Kurihara (1965) suggests another alternating-method scheme in which the leapfrog step is corrected with a trapezoidal step. The scheme is

$$\phi^* = \phi^{t-\Delta t} + 2\Delta t F(\phi^t),$$

$$\phi^{t+\Delta t} = \phi^t + \frac{\Delta t}{2}[F(\phi^*) + F(\phi^t)]$$

and is second order in time. While two function evaluations are needed per time step, the maximum allowable Courant number is 1.41; thus, larger time steps may be used and the scheme may have an efficiency comparable to leapfrog and the Magazenkov scheme. In the time splitting, the KW small-time-step scheme is used to advance the solution from $t - \Delta t$ to $t + \Delta t$ to arrive at the predictor value ϕ^* and is also used to advance the solution from t to $t + \Delta t$ in the trapezoidal step. The stability characteristics of the Magazenkov scheme and leapfrog–trapezoidal scheme are similar; thus, the scheme provides a possible alternative to leapfrog for the time-split system. Again, coding complexity appears to be the primary drawback.

No other pure time-integration scheme is known that might be suitable for a time-split model, either because the schemes require multiple function evaluations per time step or because there is no clear way to incorporate them into the time-split approach.

c. *Forward-in-time schemes for advection*

There are many forward-in-time advection schemes that could be used for the advection terms in a time-split model. The forward-in-time schemes are attractive because of the high accuracy and the possible monotonic and positive-definite characteristics possessed by many of the schemes. The schemes also allow integration of the acoustic modes in a time-split scheme from t to $t + \Delta t$, cutting in half the small-time-step computations of the leapfrog-based time-split scheme.

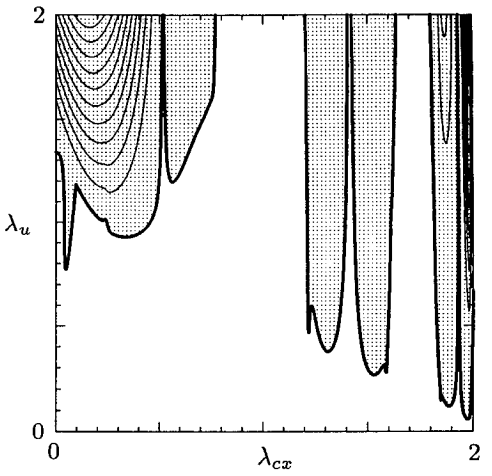

FIG. 10. Amplification factor for the explicit acoustic-advection system with the Magazenkov scheme used for advection. There are six small time steps per large time step. Contouring as in Fig. 1. The instabilities at $1.3 < \lambda_{cx} < 1.7$ are adequately damped using divergence damping.

Many of these schemes are nonlinear; thus, they cannot be considered in a linear stability analysis. A class of linear, forward-in-time schemes referred to as Crowley schemes is analyzed by Tremback et al. (1987). This section examines the second-order–accurate Crowley schemes for use in the time-split model, and comments are made on the higher-order Crowley schemes as well. The second-order–accurate Crowley scheme is

$$\phi_j^{t+\Delta t} = \phi_j^t - \frac{\alpha}{2}(\phi_{j+1}^t - \phi_{j-1}^t) + \frac{\alpha^2}{2}(\phi_{j+1}^t - 2\phi_j^t + \phi_{j-1}^t),$$

where α is the Courant number $U\Delta t/\Delta x$ or $W\Delta t/\Delta z$. Analysis of the scheme with the acoustic modes requires that the finite-difference spatial discretization be considered. The Arakawa C grid is used for the spatial discretization. The small-time-step equations (16)–(18) remain the same, but the frequencies λ must be redefined. Discretization on the C grid and Fourier decomposition in space results in a new acoustic-mode parameter:

$$\lambda_{cx} = \frac{2c_s\Delta\tau}{\Delta x}\sin\left(\frac{k\Delta x}{2}\right). \quad (40)$$

In our notation, λ_u for the Crowley scheme is

$$\lambda_u = -i\alpha^2[1 - \cos(k\Delta x)] + \alpha\sin(k\Delta x). \quad (41)$$

Replacing x with z and k with l gives the new λ_w. As with previous systems, the most stringent stability restrictions result from the advection of propagating acoustic modes, and we will set $\lambda_N = 0$ in (16)–(18).

Figure 11 depicts the stability region for $n_s = 6$ with explicit integration of the acoustic modes for the $4\Delta x$ horizontal-wavelength mode. The instabilities associated with the advection of high-frequency acoustic modes are significantly stronger for this scheme than for the leapfrog scheme (compare Figs. 11 and 1c). Divergence damping and other filters will help control the instabilities, particularly those associated with the short-wavelength horizontal modes. However, the longer-wavelength modes are also unstable, and while the instability is weaker for longer wavelengths, it covers a larger portion of the $\lambda_{cx} - \lambda_u$ stability domain. The longer-wavelength modes are not appreciably damped by most filters; hence, the use of this Crowley scheme with explicit integration of the acoustic modes is not recommended.

The stability of the higher-order Crowley schemes has been examined for use in the explicit time-split algorithm. It is found that the higher-order Crowley schemes excite weaker instabilities than their lower-order brethren. In general, the increased damping in the lower-order schemes on the large time step leads to larger instabilities associated with the advection of the acoustic modes. The higher-order Crowley schemes have less damping and smaller instabilities, and the counterintuitive result is that the scheme with less damping is more stable. Through sixth order, however, the instabilities are still more severe than those arising in the KW scheme, and the long-wavelength instabilities remain.

Results from the analysis of the Crowley schemes can be directly applied to the use of semi-Lagrangian schemes for advection in an explicit time-split approach. The stability and accuracy analysis of a semi-Lagrangian advection scheme using Lagrange polynomial interpolators is given in Bates and McDonald (1982). Consider the 1D quadratic semi-Lagrangian advection with a Courant number $\alpha = U\Delta t/\Delta x \leq 1/2$. Introducing Fourier modes into the spatially discrete system allows one to express the scheme as

$$\phi^{t+1} = \phi^t + [-\alpha^2(1 - \cos k\Delta x) - i\alpha \sin k\Delta x]\phi^t. \tag{42}$$

Equation (42) is (9) in Bates and McDonald, with $p = 0$. The parameter λ_u for the semi-Lagrangian scheme is that given by (41) in our analysis of the Crowley schemes. Thus, our first result is that the semi-Lagrangian schemes would be expected to behave like the Crowley schemes when used in the time-split approach of KW. Note that the acoustic integrations are not performed along the trajectory, and we do not know of any attempts to construct a split-explicit semi-Lagrangian model where the fast-mode integrations are performed along the trajectory.

Purser and Leslie (1991) present a time-split approach that uses semi-Lagrangian advection and is based on the traditional additive-splitting scheme but introduces a small–large time-step coupling similar to that used in KW. The notation of Purser and Leslie is used in describing the scheme. First, M small time steps (adjustment steps in Purser and Leslie) are taken to advance the fast modes:

$$u^{n,m+1} = u^{n,m} + i\lambda_{cx}p^{n,m} + M^{-1}F_{u_*}^{n-1,M}, \tag{43}$$

$$p^{n,m+1} = p^{n,m} + i\lambda_{cx}u^{n,m+1} + M^{-1}F_{p_*}^{n-1,M}, \tag{44}$$

where n is the time level and m is the number of small time steps taken at that time level. The semi-Lagrangian advection term F_u^t is defined, using (42), as

$$F_u^{t,m} = -i\lambda_u u^{t,m},$$

and likewise for F_p^t. After the small time steps, the advection used in the small time steps is subtracted out:

$$u_*^{n,M} = u^{n,M} - F_{u_*}^{n-1,M} \quad \text{and} \quad p_*^{n,M} = p^{n,M} - F_{p_*}^{n-1,M}. \tag{45a), (45b)}$$

The large time step (advection) is computed using these results:

$$u^{n+1,0} = u_*^{n,M} + F_{u_*}^{n,M} \tag{46}$$

$$p^{n+1,0} = p_*^{n,M} + F_{p_*}^{n,M}. \tag{47}$$

Note that the advected quantity used in the operator F in (43) and (44) is that recovered at the end of the previous set of small time steps and not the value resulting from the previous *complete* time step; thus, only one advection calculation is performed every time step and the result is saved for reuse on the next time step.

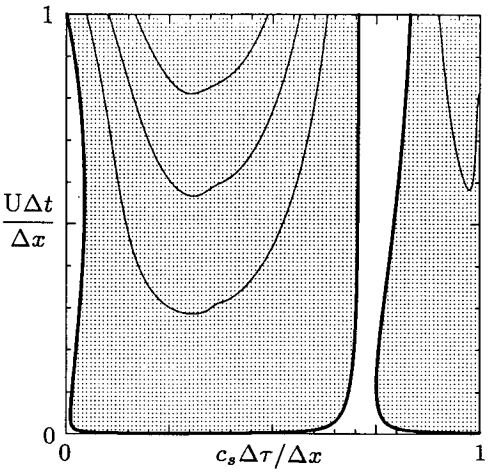

FIG. 11. Amplification factor for the explicit acoustic-advection system for the $4\Delta x$ mode with the first-order Crowley scheme used for advection. There are six small time steps per large time step.

First, we note that the scheme described above is not that given in Purser and Leslie (1991). In Purser and Leslie, the scheme is incorrectly stated in that the Lagrangian advection terms used in the small time steps [the leftmost terms in (43) and (44)] should be subtracted out *before* the large time step, as described here, as opposed to being subtracted out *after* the large time step, as described in Purser and Leslie (J. Purser, personal communication). However, the model calculations reported in Purser and Leslie were performed with the correct scheme (43)–(47).

This scheme differs from the traditional additive-splitting scheme in that a time-lagged advection is now included on the small time steps. This time-lagged advection is then subtracted from the small-time-step results before the advection step is taken. A stability analysis of this scheme shows that it possesses stability properties similar to that of the Crowley scheme used with the KW approach examined earlier in this section. Thus, the scheme does not appear to present a viable alternative to the KW scheme. Although Purser and Leslie present results from stable integrations using this scheme, filters are used in their shallow-water integrations, and they have found that their scheme is unstable for Courant numbers α greater than 1 (J. Purser, personal communication).

Implicit integration of the acoustic modes using the Crowley schemes for advection can be examined by considering the simple discrete equation

$$\phi^{n+1} = \phi^n - i\lambda_w\phi^n - \frac{i\lambda_{cz}}{2}\left(\frac{1+\beta}{2}\phi^{n+1} + \frac{1-\beta}{2}\phi^n\right), \tag{48}$$

where λ_{cz} and λ_w are given in (40) and (41), respectively, with w replacing u and z replacing x. For the second-order Crowley scheme, the amplification factor for (48) is

$$A = \frac{1 - i\lambda_w - i\lambda_{cz}(1-\beta/2)}{1 + i\lambda_{cz}(1+\beta/2)}.$$

Figure 12 shows the stability space for this scheme. Both short- and long-wavelength instabilities exist, though both are effectively damped by off centering the implicit acoustic-mode integrations. The higher-order Crowley schemes possess these same stability characteristics when coupled with implicit integration of the acoustic modes. Thus, the Crowley advection schemes can be used in models where the acoustic modes are integrated implicitly, but the acoustic integration must be off centered for stability. Also, as with any fully implicit acoustic-mode integrations, a multidimensional Helmholtz equation must be solved.

Filtering will damp the instabilities in schemes with explicit and implicit integration of the acoustic modes. Divergence damping and off centering of the vertically implicit small time step have been used with mixed results in nonlinear models where the horizontally

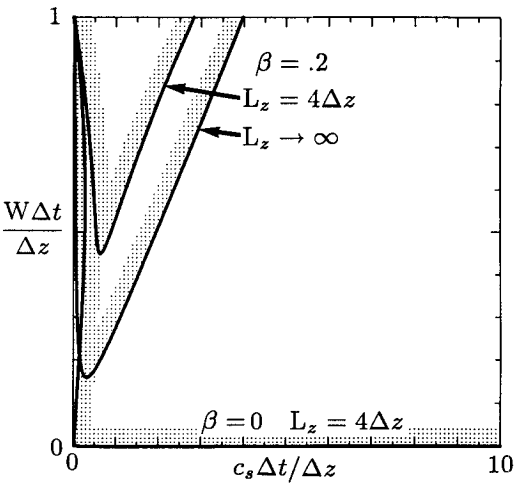

FIG. 12. Amplification factor for implicit acoustic-mode integration with the second-order Crowley scheme used for advection. There is one small time step per large time step. Contouring is as in Fig. 10.

propagating acoustic modes have been integrated explicitly. The models have not proven as stable as the leapfrog-based time-split model. Time-split models have also been constructed using the nonlinear forward-in-time scheme of Smolarkiewicz (1984), and the stability of the calculations follows that of the Crowley scheme, that is, filtering is needed and calculations are often unstable. In general, hybrid models have shown the most success where forward-in-time schemes are used (L. Wicker, personal communication); the hybrid models advance the scalars with the forward-in-time scheme, and momentum is handled with the traditional leapfrog scheme.

6. Conclusions

Both the hydrostatic and nonhydrostatic elastic equations can be solved using the same time-split numerical methods. In our analysis of explicit time-split numerical methods, where no multidimensional elliptic equation need be solved, we conclude that the leapfrog-based time-split method of KW is the most appropriate for integrating the hydrostatic or nonhydrostatic systems. All other schemes possess some greater drawback; for example, schemes are less stable, require excessive damping for reasonable stability, or significantly increase code complexity. In particular, the method of Madala (1981) can be viewed as a more complex extension of KW that does not increase accuracy or stability. As outlined by McGregor (1987) and Purser and Leslie, additive-splitting techniques can result in noisy solutions, and while they have been used in hydrostatic computations, they are not used in nonhydrostatic models.

Forward-in-time advection schemes have been analyzed for their use in a KW time-split model. These schemes excite instabilities associated with the advec-

tion of acoustic modes and, for the Crowley schemes analyzed with explicit integration of the acoustic modes, the instabilities tend to be much larger than those associated with the leapfrog scheme. These instabilities grow smaller in the higher-order schemes. In particular, use of the Crowley schemes excite a long horizontal-wavelength instability that is not easily damped using standard filters. These observations, and tests with nonlinear models, strongly suggest that the Crowley schemes are unsuitable for use in an explicit time-split model based on a KW-type small time step with a forward-in-time slow-mode integration. This result is likely to apply to many other forward-in-time advection schemes. Purser and Leslie's (1991) method, which makes use of forward-in-time semi-Lagrangian advection in an additive-splitting approach that incorporates a small–large time-step coupling in some ways similar to that in KW, does not improve on the generally poor stability of the split-explicit forward-in-time schemes.

We have introduced two extensions to the original KW scheme to improve its performance. First, an acoustic filter is described that eliminates the need for strong Robert filtering of the solution. The new filter, which we refer to as divergence damping, also removes the need for off centering the vertically implicit acoustic integration in KW, introduced by DK to damp numerical instabilities in cases possessing strong mean atmospheric stability. Divergence damping is preferable to other forms of damping because it only damps divergent modes; it leaves gravity waves largely unaffected. Second, we have presented a scheme wherein the vertical advection of buoyancy and the buoyancy term in the vertical-momentum equation are handled implicitly on the small time step. This scheme, used by Cullen (1990) and Tanguay et al. (1990) in semi-implicit nonhydrostatic models, removes all stability restrictions based on the Brunt–Väisälä frequency and leaves the large time step restricted by the advection velocity and the small time step restricted by the horizontal sound-wave velocity.

It is possible to use a greater variety of advection schemes in conjunction with implicit integration of the acoustic and/or gravity-wave terms. The implicit schemes coupled with leapfrog integration of the slow modes are very stable and are used successfully in many hydrostatic and nonhydrostatic models. When an implicit fast-mode integration scheme is used with the Crowley, semi-Lagrangian, and other forward-in-time advection schemes, short- and long-wavelength instabilities exist that are not present in the leapfrog-based schemes. Moderate off centering of the implicit acoustic-mode integration does damp the instabilities, as does divergence damping in both hydrostatic and nonhydrostatic models. Thus, implicit integration of the fast modes is an attractive alternative to the split-explicit approaches. However, one must solve a multidimensional elliptic equation when using an implicit method.

The major portion of this paper focuses on the stability of explicit time-split integration schemes with the general result being that at least some minimal filtering is always necessary. The stability of implicit methods has also been examined where convenient, and it has been found that these methods generally require less filtering for stability than their split-explicit counterparts. However, in actual nonlinear applications, especially when using real data, the filtering used in split-explicit models is generally no more than that used in the implicit models. Also, in nonhydrostatic applications, the acoustic filter described previously selectively damps the acoustic modes, while the Robert time filter and the off centering of implicit schemes damps all high-frequency modes. Thus, the relative merits of split-explicit and implicit approaches should focus on relative numerical efficiency and simplicity. In terms of CPU time needed on present-day machines, we have found the computational costs of the two methods to be roughly equivalent for general atmospheric flow simulations (though in specific applications one scheme may be more economical than the other).

We also note that machine architectures are changing rapidly, and algorithms that work well on existing serial computers may not work well on massively parallel computers. In particular, while it appears that the split-explicit schemes will map well onto the new massively parallel architectures, it is not obvious how to efficiently solve elliptic equations on the massively parallel machines. Further evaluation of the different schemes awaits future hardware/software and algorithm development.

Acknowledgments. The first author was partially funded under NSF Grant ATM 8809862.

APPENDIX

The von Neumann stability analysis, as described in Roache (1972, pp. 42–45), requires that the discrete system (21) and (22) be written as a matrix equation of the form $\phi^{t+\Delta t} = A\phi^t$. The matrix $\mathbf{A}$ is the amplification matrix, and for stability its eigenvalues must have an absolute value of less than or equal to one. Analysis of the small–large time-step coupling requires that the full time step be contained in the matrix $\mathbf{A}$: that is, the large time step, n_s small time steps, and any filtering.

A full time step, (21) and (22) with Robert filtering, can be represented as follows:

$$\mathbf{u}^{t+\Delta t} = \mathbf{F}\mathbf{S}^{n_s}\mathbf{L}\mathbf{u}^t,$$

where

$$\mathbf{u}^t = [u^\tau, p^\tau, u^t, p^t, u^{t-\Delta t}, p^{t-\Delta t}]^{\mathrm{T}}.$$

The square matrices **L**, **S**, and **F** represent the large time step, small time step, and Robert filter–variable reset, respectively, and are order 6. The time step can be written in more compact form, but this form mirrors the actual computation in that in the typical model the large time step is taken first, followed by n_s small time steps, and finally a Robert filter and a resetting of the variables. At the beginning of a time step, $\phi^\tau = \phi^{t-\Delta t}$. In this example, the large-time-step matrix is the identity matrix because no variable is advanced on the large time step. If buoyancy was included as in (15), it would be advanced with the application of the matrix **L**. The matrices **S** and **F** are

$$\mathbf{S} = \begin{pmatrix} 1 & -i\lambda_{cx} & -i\lambda_u/n_s & 0 & 0 & 0 \\ -i\lambda_{cx} & 1-\lambda_{cx}^2 & -\lambda_{cx}\lambda_u/n_s & -i\lambda_u/n_s & 0 & 0 \\ 0 & 0 & 1 & 0 & 0 & 0 \\ 0 & 0 & 0 & 1 & 0 & 0 \\ 0 & 0 & 0 & 0 & 1 & 0 \\ 0 & 0 & 0 & 0 & 0 & 1 \end{pmatrix}$$

$$\mathbf{F} = \begin{pmatrix} \alpha & 0 & 1-2\alpha & 0 & \alpha & 0 \\ 0 & \alpha & 0 & 1-2\alpha & 0 & \alpha \\ 1 & 0 & 0 & 0 & 0 & 0 \\ 0 & 1 & 0 & 0 & 0 & 0 \\ \alpha & 0 & 1-2\alpha & 0 & \alpha & 0 \\ 0 & \alpha & 0 & 1-2\alpha & 0 & \alpha \end{pmatrix}.$$

For the von Neumann analysis, $\mathbf{A} = \mathbf{F}\mathbf{S}^{n_s}\mathbf{L}$. The subroutine CG is used in the EISPACK software library on the NCAR CRAY Y-MP8/64 to find the eigenvalues of the matrix **A**. All von Neumann stability analyses presented in this paper are computed in this manner.

It should be noted that in cases where there is more than one eigenvalue of the matrix **A** equal to 1, the stability condition that all the eigenvalues of the matrix have an absolute value of less than or equal to 1 is a necessary, though not a sufficient, condition. A sufficient, though not necessary, condition for stability in these cases is that the spectral norm of the matrix **A** be less than or equal to 1. The lack of sufficiency arises because the spectral radius of **A** (its largest absolute eigenvalue) is used to approximate the spectral norm of **A**. We have checked our stability results and found that the spectral radius is a good approximation to the spectral norm in the cases presented. A detailed analysis of the stability requirements is given in Sod (1985), along with examples where the spectral radius does not accurately approximate the spectral norm.

REFERENCES

Asselin, R. A., 1972: Frequency filter for time integrations. *Mon. Wea. Rev.*, **100,** 487–490.

Burridge, D. M., 1975: A split semi-implicit reformulation of the Bushby–Timpson 10-level model. *Quart. J. Roy. Meteor. Soc.*, **101,** 777–792.

Bates, J. R., 1984: An efficient semi-Lagrangian and alternating direction implicit method for integrating the shallow water equations. *Mon. Wea. Rev.*, **112,** 2033–2047.

——, and A. McDonald, 1982: Multiply-upstream, semi-Lagrangian advective schemes: Analysis and application to a multi-level primitive equation model. *Mon. Wea. Rev.*, **110,** 1831–1842.

Carpenter, K. M., 1979: An experiment using a nonhydrostatic mesoscale model. *Quart. J. Roy. Meteor. Soc.*, **105,** 629–655.

Chao, W. C., 1982: Formulation of an explicit-multiple-timestep time integration method for use in a global primitive equation grid model. *Mon. Wea. Rev.*, **110,** 1603–1617.

Clark, T. L., 1977: A small scale dynamic model using a terrain following coordinate transformation. *J. Comput. Phys.*, **24,** 186–215.

——, 1979: Numerical experiments with a three-dimensional cloud model: Lateral boundary condition experiments and multi-cellular severe storm simulations. *J. Atmos. Sci.*, **24,** 186–215.

Cullen, M. J. P., 1990: A test of a semi-implicit integration technique for a fully compressible non-hydrostatic model. *Quart. J. Roy. Meteor. Soc.*, **116,** 1253–1258.

Deardorff, J. W., 1974: Three-dimensional numerical study of the height and mean structure of a heated planetary boundary layer. *Bound.-Layer Meteor.*, **7,** 81–106.

Droegemeier, K. K., and R. B. Wilhelmson, 1987: Numerical simulation of thunderstorm outflow dynamics. Part I: Outflow sensitivity experiments and turbulence dynamics. *J. Atmos. Sci.*, **44,** 1180–1210.

Durran, D. R., 1991: The third-order Adams–Bashforth method: An attractive alternative to leapfrog time differencing. *Mon. Wea. Rev.*, **119,** 702–720.

——, and J. B. Klemp, 1983: A compressible model for the simulation of moist mountain waves. *Mon. Wea. Rev.*, **111,** 2341–2361.

Gadd, A. J., 1978: A split explicit integration scheme for numerical weather prediction. *Quart. J. Roy. Meteor. Soc.*, **104,** 569–582.

Golding, B. W., 1987: Short range forecasting over the United Kingdom using a mesoscale forecasting system. *Proc. WMO/IUGG Numerical Weather Prediction Symposium,* Tokyo, WMO.

Hill, G. E., 1974: Factors controlling the size and spacing of cumulus clouds as revealed by numerical experiments. *J. Atmos. Sci.*, **30,** 1672–1690.

Ikawa, M., 1988: Comparison of some schemes for nonhydrostatic models with orography. *J. Meteor. Soc. Japan,* **66,** 753–776.

Klemp, J. B., and R. Wilhelmson, 1978: The simulation of three-dimensional convective storm dynamics. *J. Atmos. Sci.*, **35,** 1070–1096.

Kwizak, M., and A. Robert, 1971: A semi-implicit scheme for grid point atmospheric models of the primitive equations. *Mon. Wea. Rev.*, **99,** 32–36.

Kurihara, Y., 1965: On the use of implicit and iterative methods for the time integration of the wave equation. *Mon. Wea. Rev.*, **93,** 33–46.

Leveque, R. J., and J. Oliger, 1983: Numerical methods based on additive splittings for hyperbolic partial differential equations. *Math. Comput.*, **40,** 469–497.

Madala, R. V., 1981: Efficient time integration schemes for atmosphere and ocean models. *Finite-difference Techniques for Vectorized Fluid Calculations,* D. Book, Ed., Springer-Verlag, 56–74.

Magazenkov, L. N., 1980: *Trudy glavnoi geofizicheskoi observatorii.* (Transactions of the main geophysical observatory), **410,** 120–129.

Marchuk, G. I., 1974: *Numerical Methods in Weather Prediction.* Academic Press, 277 pp. [Russian ed., 1967]

McGregor, J. L., 1987: Accuracy and Initialization of a two-time-level split semi-Lagrangian model. *Proc. WMO/IUGG Numerical Weather Prediction Symposium,* Tokyo.

Mesinger, F. M., 1977: Forward–backward scheme, and its use in a limited area model. *Contrib. Atmos. Phys.*, **50,** 200–210.

Moeng, C., 1984: A large-eddy simulation model for the study of planetary boundary-layer turbulence. *J. Atmos. Sci.*, **41,** 2052–2062.

Morel, P., and O. Talagrand, 1974: Dynamic approach to meteorological data assimilation. *Tellus,* **26,** 334–343.

Peaceman, D. W., and H. H. Rachford, 1955: The numerical solution

of parabolic and elliptic equations. *J. Soc. Indust. Appl. Maths.*, **3,** 28–41.

Polavarapu, S. M., and W. R. Peltier, 1990: The structure and nonlinear evolution of synoptic-scale cyclones: Life cycle simulations with a cloud-scale model. *J. Atmos. Sci.*, **47,** 2645–2672.

Purser, R. J., and L. M. Leslie, 1991: Reducing the error in a time-split finite-difference scheme using an incremental technique. *Mon. Wea. Rev.*, **119,** 578–585.

Ramshaw, J. D., and V. A. Mousseau, 1990: Accelerated artificial compressibility method for steady-state incompressible flow calculations. *Comp. Fluids,* **18,** 361–367.

Robert, A. J., 1966: The integration of a low order spectral form of the primitive meteorological equations. *J. Meteor. Soc. Japan,* **44,** 237–245.

Roache, P. J., 1972: *Computational Fluid Dynamics.* Hermosa Publishers, 446 pp.

Sadourny, R., 1975: The dynamics of finite-difference models of the shallow water equations. *J. Atmos. Sci.*, **32,** 680–689.

Schlesinger, R. E., 1978: A three-dimensional numerical model of an isolated thunderstorm. Part 1: Comparative experiments for variable ambient windshear. *J. Atmos. Sci.*, **35,** 690–713.

Simmons, A. J., B. J. Hoskins, and D. M. Burridge, 1978: Stability of the semi-implicit method of time integration. *Mon. Wea. Rev.*, **106,** 405–412.

Smolarkiewicz, P. K., 1984: A fully multidimensional positive definite advective transport algorithm with small implicit diffusion. *J. Comput. Phys.*, **54,** 325–362.

Snyder, C., W. C. Skamarock, and R. Rotunno, 1991: A comparison of primitive equation and semigeostrophic simulations of baroclinic waves. *J. Atmos. Sci.*, **48,** 2179–2194.

Sod, G. A., 1985, *Numerical Methods in Fluid Dynamics.* Cambridge University Press, 446 pp.

Strang, G., 1968: On the construction and comparison of difference schemes. *SIAM J. Numer. Anal.*, **5,** 506–517.

Tanguay, M., A. Robert, and R. Laprise, 1990: A semi-implicit semi-Lagrangian fully compressible regional forecast model. *Mon. Wea. Rev.*, **118,** 1970–1980.

Tapp, M. C., and P. W. White, 1976: A non-hydrostatic mesoscale model. *Quart. J. Roy. Meteor. Soc.*, **102,** 277–296.

Tatsumi, Y., 1983: An economical explicit time integration scheme for a primitive model. *J. Meteor. Soc. Japan,* **61,** 269–287.

Tremback, C. J., J. Powell, W. R. Cotton, and R. A. Pielke, 1987: The forward-in-time upstream advection scheme: Extension to higher orders. *Mon. Wea. Rev.*, **115,** 540–555.